European Journal of Applied Sciences – Vol. 13, No. 05
Publication Date: September 16, 2025
DOI:10.14738/aivp.1305.19378.
Swatland, H. J. (2025). Reviewing the Control of Meat *p*H and Light Scattering in Model Systems. *European Journal of Applied Sciences, Vol - 13(05).* 117-127.

Reviewing the Control of Meat *p*H and Light Scattering in Model Systems

Howard J. Swatland
Department of Animal Biosciences, University of Guelph

ABSTRACT

This review explains how a computer controlled system was developed to perfuse individual meat muscle fibres with phosphate buffer to change their *p*H. Fibres were mounted on a frame in an optical cell on a polarizing microscope to measure their birefringence. As *p*H was decreased, birefringence was increased. X-ray diffraction showed that this was caused by thick and thin myofilaments in the fibres moving closer together laterally. Small disks of intact muscle were measured in a macroscopic system to show that a decrease in *p*H caused an increase in reflectance. When *p*H was increased, reflectance decreased. These model systems explain how living muscle usually gets brighter as it becomes meat.

INTRODUCTION

The acidity of meat affects light scattering with a detectable effect on meat colour, which is important in consumer purchasing preferences. Lost in the vast literature on this subject in journals unlikely to be read by meat scientists are some key discoveries reviewed here. Empirical studies on vast populations of commercial meats may be commercially important, but they do not explain the basic mechanisms involved. Basic mechanisms are best investigated by controlled experiments, and model systems offer a good chance at this.

The first paper reviewed explains how *p*H may be controlled using continuous perfusion of muscle fibres with phosphate buffer [1]. This is not a perfect model system because the buffer is bound to flush away many soluble components of the sarcoplasm, particularly chromophores such as myoglobin derivatives. But it does leave myofibrils within fibres behaving in a logical manner as the *p*H changes both the lateral separation of myofilaments and light scattering. It also allows *p*H related changes to be reversed back to a point very close to the starting point. The key advantage of model systems is that they minimize biological sampling error.

The next papers reviewed use polarized light microscopy and x-ray diffraction to show how interfilament separation determines light scattering [2-4]. As *p*H declines post mortem while glycogen is converted to lactate, myofilaments decrease their lateral separation, birefringence is increased and light scattering is increased so that the dark colour of living muscle becomes the bright colour of meat we hope to find displayed on a meat counter. The final paper reviewed shows that small samples of bulk meat follow the conclusions reached by microscopy and x-ray diffraction [5].

CONTROLLING *p*H

The *p*H of phosphate buffer in a small chamber mounted on the stage of a polarizing microscope was controlled by computer. The chamber had inlet and outlet tubes, with the top of the chamber

closed by a cover glass. Fluid reservoirs for buffer stock solutions and a mixing sump were located below the microscope, from which the buffer was pumped to a small reservoir above the microscope stage, using reservoir height to control the delivery rate to the chamber. The key point was not to have any large volumes of fluid over electrical components. The *p*H of the buffer was controlled using solenoid valves for acid, base and exit valves. Other valves were used to isolate the sample chamber when optical measurements were made (otherwise fluid movement would have affected optical measurements). Iterative procedures were used to reach a target *p*H. Operational results were included in the control algorithm by updating stored values for the apparent fluid volume of the system when increasing and decreasing in *p*H – so the control system was learning as it progressed.

The working distance between the specimen and the microscope objective is difficult in a system like this, because the numerical aperture (NA) is reduced as the working distance is increased. Only a microscope cover glass was used above the sample chamber, and this became a sensitive barometer to changes in hydrostatic pressure caused by valve operation. When the valves were opened the pressure in the chamber caused the cover glass to bulge outwards or leak but, when the valves were shut, the cover glass bulged inwards and air bubbles were sometimes sucked in.

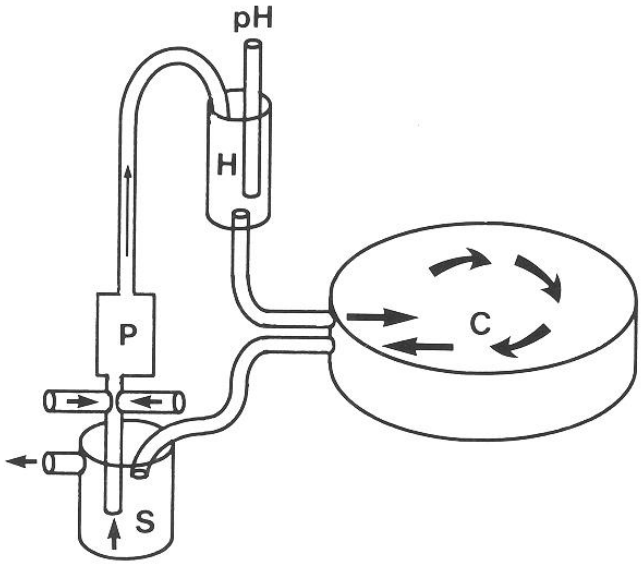

Fig 1: Fluid from a sump (S) was moved by a pump (P) to a header tank (H) containing a *p*H electrode (pH), and then passed through the specimen chamber (C) on the microscope stage [1].

The overall plan of the system is shown in Fig. 1. A small header tank (Fig. 1, H), temporarily holding a few ml of fluid, was located 10 cm above the level of the microscope stage with the specimen chamber (Fig. 1, C). Buffer was pumped to the header tank from a sump (Fig. 1, S). The flow rate through the chamber (0.5 ml min^{-1}) was determined by the tubing diameter after the header tank, the depth of fluid in the header tank, and the height of the header tank above the stage. Changes in *p*H were created by opening solenoid valves in supply lines to the pump intake, so that pump stroke volume determined the volume of fluid admitted per second of valve open time (0.16 sec ml^{-1}). The relative heights of reservoir valves above the sump were balanced so that hydrostatic pressure in the reservoir tanks had a minimal effect on the time:volume relationship of valves, or back-flow into the sump between pump cycles. Excess fluid was lost through the

overflow from the sump. Fluid *p*H was monitored from an electrode in the header tank (Fig. 1). A stainless steel mesh was located on the floor of the header tank to remove bubbles. Fluid volume in the system monitored by a depth detector was maintained so that the fluid level did not drop below this mesh once the system was in operation.

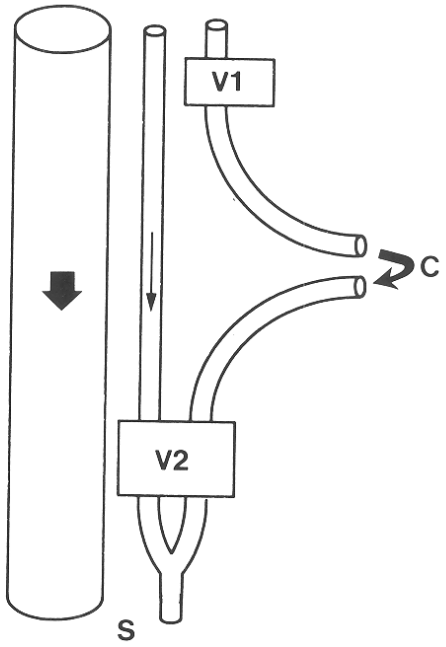

Fig 2: Details of tubing between the header tank and sump (S), allowing fluid to by-pass the specimen chamber (C) which could be isolated by valves, V1 and V2 [1].

Figure 2 shows the location of additional tubes and valves. A large diameter (ID = 7 mm) tube from the header tank to the sump (Fig. 2, S) reduced the pressure fluctuations in the specimen chamber as well as reducing cycling times and increasing fluid mixing. With its upper opening above the level of the de-bubbling mesh, it acted as an overflow for the header tank. A continuous flow cell Abbe refractometer was in series with this tube, with the flow cell as a "U" bend trap.

Isolation of the specimen chamber was required when optical measurements were made, using two solenoid valves (Fig. 2, V1 and V2), to prevent moving fluid from causing small movements of the specimen. Isolation of the chamber ensured that the cover glass was flat. The upper valve, V1, was a simple shut off. The lower valve, V2, was a two-way valve that shut-off the specimen chamber but opened a small-diameter flushing tube. An exit valve was used after the pump to reduce wastage and facilitate calculations. The header tank and sump both had high-level detectors that generated non-maskable interrupts to the computer. The specimen chamber had two tubes for the inlet and outlet of fluid. Both were adjacent to create a circular flow of fluid around the chamber. An air-bubble created when the specimen was first sealed into the chamber, was removed when valves V1 and V2 were opened, the slide was tilted with inlet and outlet tubes uppermost. The specimen was secured to a small metal frame just under the cover glass. With Sørensen's phosphate buffer, programming *p*H was reduced to balancing the volumetric ratios of equimolar solutions of dibasic sodium phosphate and monobasic potassium phosphate. Fig. 3 shows an example of a programmed pH change, from pH 6 to 7. The status of acid (A), base (B), and exit (E) valves is shown in the upper part of the figure.

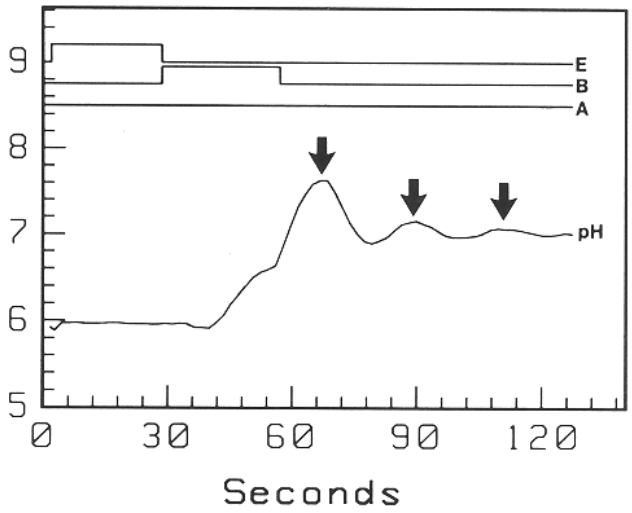

Fig 3: A one-shot programmed change from pH 6 to 7, showing the status of acid (A), base (B), and exit (E) valves [1].

Direct calculation and one-shot changes were not reliable in practice where the volumes of moving and replaced fluid were known only approximately. A wait between changing the pH and measuring the specimen was required, to be sure that equilibration has occurred within the specimen, so an iterative procedure was more robust, whereby a series of low estimates led to the required pH, as shown in Fig. 4, for a programmed change from pH 7 to 5.5. As seen from the valve status in the upper part of Fig. 4, fluid was only dumped from the exit valve for the first two replacements by acid salt solution, so that the effect of the third addition was weakened to give some fine-tuning. Although sacrificing speed of change, iterative procedures had many advantages over one-shot solutions. It is not necessary to know the exact chemical nature or dilutions of the buffer stock solutions, which facilitated preparation of large volumes of stock fluids. The first addition of acidic or basic components was used to interrogate the system, finding the magnitude of the response for a known change, and allowing the development of a simple expert system. But the target for the iterative procedure had to be defined as an acceptance window rather than an exact value, otherwise the target was never attained and the system oscillated.

In Fig. 4, for example, the first two openings of the acid valve were for fluid replacement and were called from step 2, while the third opening was for fluid addition and was called from step 7. Using the small-diameter tube that by-passed the specimen chamber when it was isolated (Fig. 2), often it was possible to do two things simultaneously: (1) internal equilibration and optical measurement of the specimen at a previous *p*H, and (2) change the remainder of the system to the next *p*H. Near the middle of the buffering range, reconnection of the specimen chamber to the system caused only a small change in pH, which usually was within the acceptance window. When the *p*H was changed from 5.5 to 7 there was a small increase in the refractive index (RI) of the buffer (from 1.3330 to 1.3342) but with a minimal effect on subsequent optical measurements.

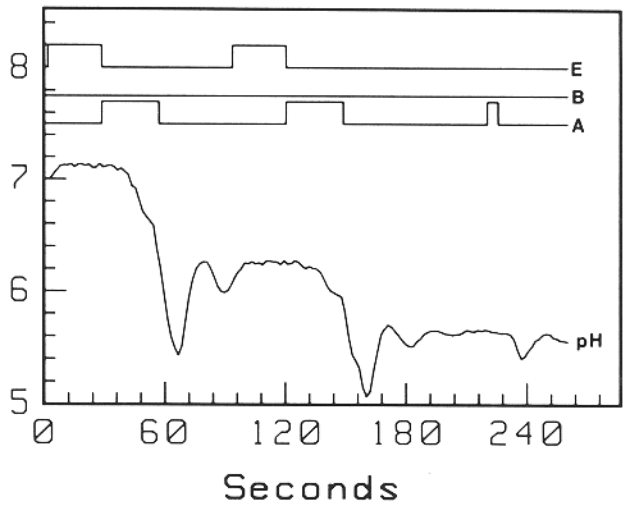

Fig 4: An iterative procedure to change the pH from 7 to 5.5, showing the status of acid (A), base (B), and exit (E) valves [1].

BIREFRINGENCE

The development of an automated *p*H changer made it possible to automate microscopic measurements on single muscle fibres to prove that *p*H changes birefringence and then light scattering and then meat colour. A quarter-wave plate was used to measure the small path differences between the two refractive pathways through muscle fibres [3]. This method of ellipsometry was invented in 1840 by de Sénarmont [6] for light reflected from minerals, and much later adapted for transmitted light by Goranson and Adams [7]. Poincaré diagrams for the method are given by Hartshorne and Stuart [8]. A de Sénarmont compensator was oriented diagonally NW-SE below the analyzer so that the final orientation of the slow axis was N-S.

To use a quarter-wave plate to measure birefringence, (1) the plate was oriented under the polarizer in N-S and analyzer in E-W directions, (2) the muscle fibre was rotated to its extinction position, (3) then rotated 45^{o} to SW-NE diagonal, (4) then the de Sénarmont compensator was inserted, (4) the wavelength was set to 589 nm (for which the plate was calibrated) , (5) then, starting at 90^{o}, the positive angle was found through which the analyzer was turned to re-find the extinction of the sample, and (6) and results were checked against a Michel-Lévy color chart. A calcite tilting compensator, was used to show that the slow optical axis of the muscle fibre was parallel to the long axis of the fibre (positive birefringence), as required for the initial selection of the fibre orientation.

Although the subjective determination of an extinction position may be fairly reliable in the case of a single static sample, problems arise when the sample is slowly changing with a *p*H controller. Thus, the operator may be biased in some way by an anticipated change. The first stage of automation was to make an objective decision on the extinction position by collecting two data vectors, one corresponding to the resistance of a potentiometer geared to the analyzer and the other corresponding to the output of the photometer. A measuring aperture corresponding to about one quarter of the muscle fibre diameter was used. Finally, the rotation of the analyzer was automated by the device shown in Fig 5. The jaws of a clamp were used to turn the analyzer.

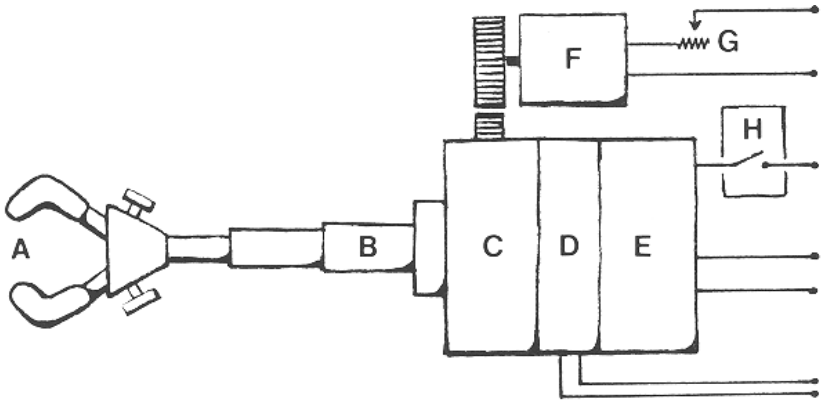

Fig 5: Apparatus to rotate an analyser. Jaws to grip the knob of the analyser, A; telescopic shaft, B; variable-speed gear box, C; electric clutch, D; reversible motor, E; multiturn potentiometer, F; adjustment potentiometer, G; and limit switches, H [2].

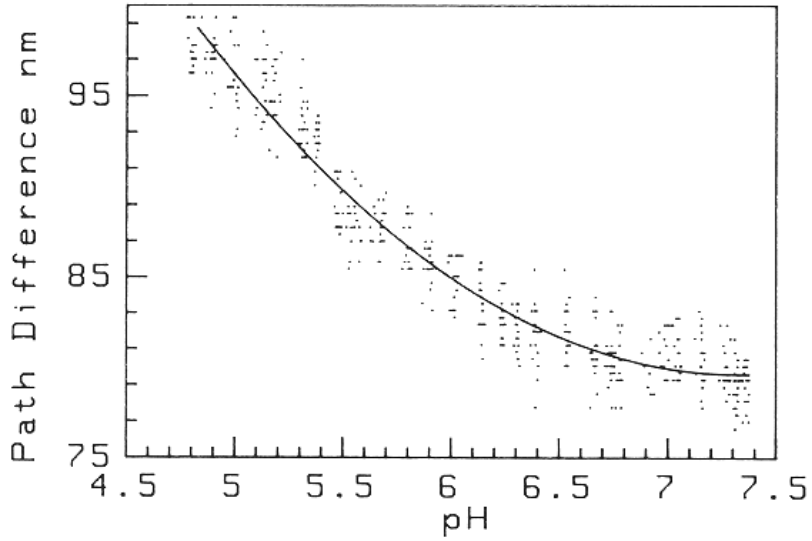

Fig 6: Path difference of birefringence in relation to pH [2].

The data in Fig. 6 show an automated *p*H decline in a *psoas minor* muscle fibre. It took a couple of hours to take the sample from an abattoir, dissect it, mount it under the microscope, standardize the optics and then start the *p*H controller to drop the *p*H in a pattern to be expected in the source material (-0.05 *p*H min^{-1}). This begs an obvious question, how might a change in birefringence be related to the common knowledge that meat usually becomes brighter in colour after slaughter (unless there is no glycogen as a substrate for glycolysis). When this research was in progress, there was no experimental evidence to explain how a decrease in *p*H might cause an increase in light scattering in meat. Biochemists had made admirable progress in exploring the molecular structure of skeletal muscle and its conversion to meat, but even authoritative text books offered nothing more than some simplistic opinions about the common knowledge that a decline in meat *p*H was always accompanied by an increase in light scattering, from the dark translucency of living muscle to the bright colours of meat. Using diagrams from blackboards using chalk and given in countless lectures when I was still teaching, here is how we get from micro optics to meat colour (Fig. 7).

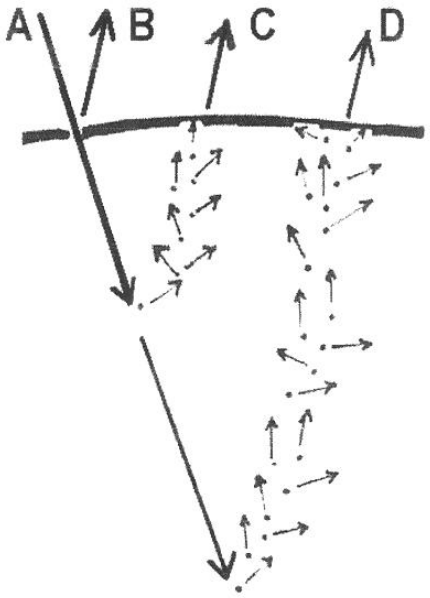

Fig 7: An old teaching diagram to explain light interacting with bulk meat.

Incident light illuminates the meat (Fig. 7, A), some of it is reflected from the wet surface (Fig. 7, B), and the remainder passes into the meat. Each little dot in the diagram represents something that scatters the light. Two possible pathways are shown, a short one with high scattering (Fig. 7, C) and a long one with low scattering (Fig. 7, D). For the short pathway, much of the light is scattered back to the surface where it is visible to the observer, but there has been little selective absorbance by soluble meat pigments between the sources of scattering, so the meat appears bright or pale. For the long pathway, much less light gets back to the meat surface and there has been high absorbance by meat pigments, so the meat appears darkly coloured. Figure 8 shows the possibilities for light that penetrates a muscle fibre to interact with myofibrils inside the fibre.

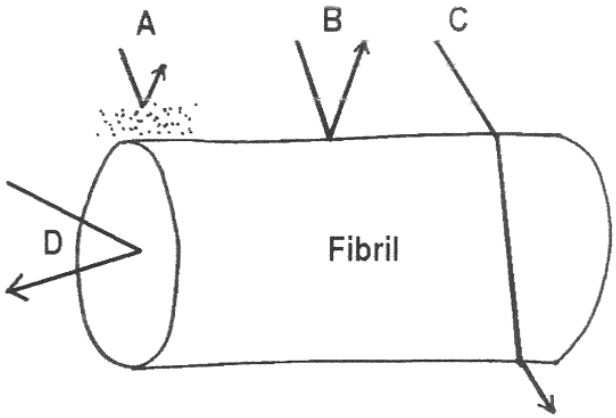

Fig 8: The next old teaching diagram considering light on a myofibril inside a muscle fibre. Light may be scattered by precipitated sarcoplasmic proteins on the surface of the myofibril (A), or reflected from the surface of the myofibril (B), or refracted through the myofibril (C), or reflected by sarcomere disks within the myofibril where interference may cause iridescence.

From a lateral view of a myofibril, it may not be immediately obvious how an increase in refraction (Fig. 8, C) is going to increase the light returned to the surface of the meat (Fig. 7, C). The answer is in a cross section (Fig.8).

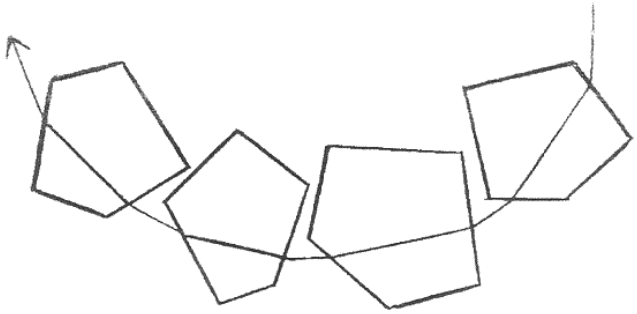

Fig 9: Yet another teaching diagram of myofibrils inside a muscle fibre seen in cross section.

This was always a difficult diagram to draw with chalk on a blackboard, making the angle changes on the surface of the myofibrils correct. Myofibrils seldom have such flat surfaces in cross section, although some do. The key point is that the incident light coming in from the right side of the diagram has been turned 180° to return to the meat surface, as in Fig. 7, C. So, this is how we get from refractive index to meat paleness, and give thanks that myofibrils are birefringent, otherwise this would be very difficult to prove experimentally. The emphasis in this review is on birefringence, leaving aside all the other possibilities (Fig. 8, A, B and D) that may proven by using polarized light, each worthy of a separate review.

FILAMENT SPACING

What causes birefringence in myofibrils? This may be answered by x-ray diffraction to look at the lateral separation of myofilaments within myofibrils.

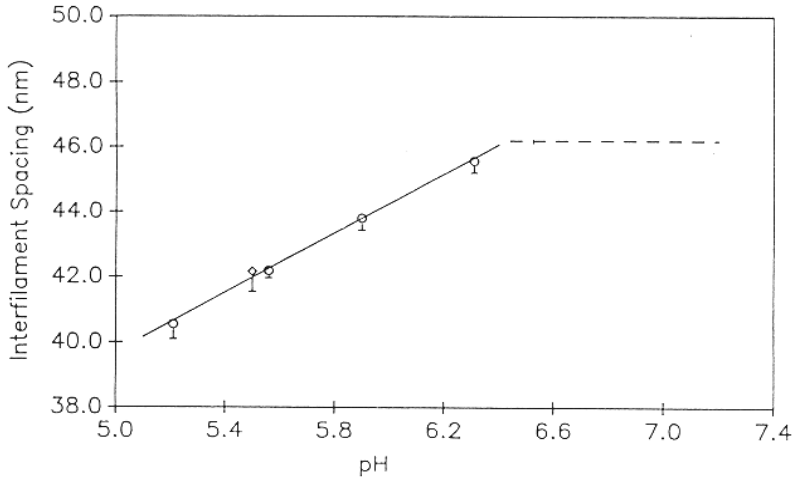

Fig 10: X-ray diffraction showing interfilament separation in pork as a function of controlled *p*H in a model system. The open circles with error bars approach a broken line determined by previous measurements in pork carcasses [4]

As *p*H declines in a model system, the myofilaments move closer together and increase the refractive index of myofibrils (Fig. 10). X-ray diffraction in meat is usually a model system because the meat samples are equilibrated to buffer solutions, and recording the diffraction patters takes quite a long time. Strong synchrotron x-ray illumination is much faster in basic research but may not yet have been used for meat?

BULK MEAT

These microscopic and submicroscopic data may be interesting, but do they match up to what may be measured in bulk meat? In the apparatus to control the *p*H of bulk meat in a model system (Fig. 11), the key part was a stainless steel mesh (Fig. 11, S) to trap the meat sample (Fig. 11, M). Buffer fluid with a controlled *p*H was pumped above and below the grid (Fig. 11, F). Optical changes in the meat sample were measured by fibre optics below the sample (Fig. 11, L). Some of the optical fibres illuminated the meat, while others captured reflected light.

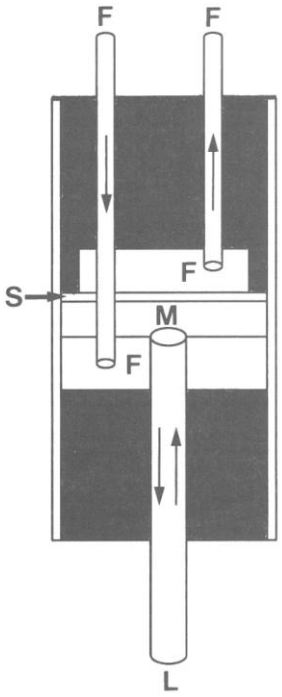

Fig 11: A sample chamber to measure how *p*H changes affect the reflectance of pork [5].

A programmed *p*H change for a disk of bulk pork is shown in Fig. 12. The reflectance dip around 530 nm was caused by myoglobin. Changes in this region were caused by the myoglobin being flushed out, although leaving Soret band absorbance by trapped mitochondria. The most convincing evidence of this refractive effect on reflectance was that it could be reversed by increasing the *p*H (Fig. 13). There were some changes in the shapes of reflectance spectra, not surprising with continuous flushing with phosphate buffer almost certainly removing other proteins. But the refractive effects of *p*H on reflectance in bulk meat matched the effects observed in individual muscle fibres. A reversible refractive effect was detected in pale, soft, exudative pork but there were other things involved [5].

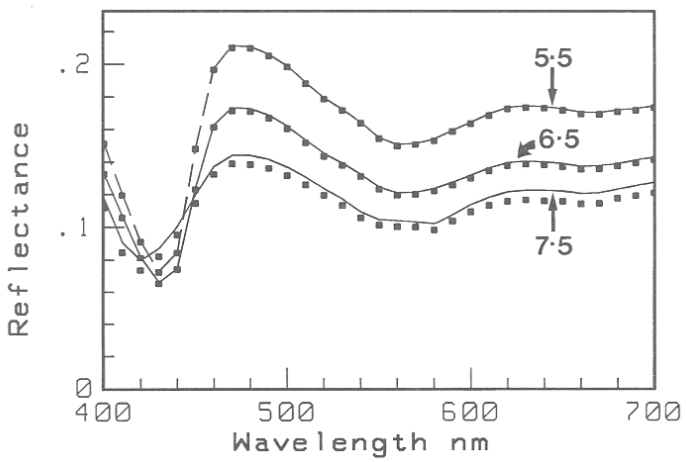

Fig 12: A programmed change from *p*H 7.5 to 5.5 in a disk of pork *transversus abdominis*. The line shows the mean of 10 replicates and the solid squares show one standard deviation subtracted from the mean [5].

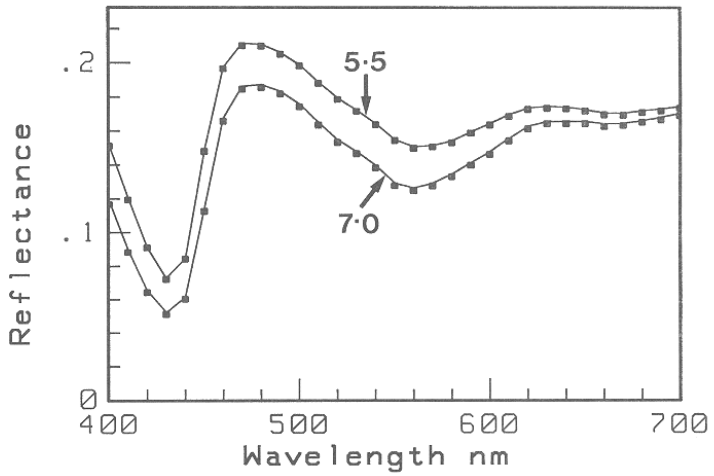

Fig 13: The disk of pork in Fig 12 subjected to an increase in *p*H. The line shows the mean of 10 replicates and the solid squares show one standard deviation subtracted from the mean [5].

CONCLUSION

Until superseded by newer research, these old data and their interpretation still provide a credible explanation for how postmortem glycolysis with a decrease in meat *p*H is responsible for colour changes as living muscle is converted to meat. Refractive changes are only part of the story, leaving precipitation of sarcoplasmic proteins, reflective changes of membranes and myofibrillar surfaces, and the reflective contribution from sarcomere disk interference to be proven (Fig. 8). Model systems offer the best hope of doing this.

References

[1] Swatland, H.J. (1994). Program control of changes in the pH of biological specimens for light microscopy. Journal of Computer-Assisted Microscopy 6: 41-46.

[2] Swatland, H.J. (1989). Birefringence of beef and pork muscle fibers measured by scanning and ellipsometry with a computer-assisted polarizing microscope. Journal of Computer-Assisted Microscopy 1: 249-262.

[3] Swatland, H.J. (1990). Effect of pH on the birefringence of skeletal muscle fibers measured with a polarizing microscope. Transactions of the American Microscopical Society 109: 361-367.

[4] Irving, T.C., Swatland, H.J. and Millman, B.M. (1990). Effect of pH on myofilament spacing in pork measured by x-ray diffraction. Canadian Institute of Food Science and Technology Journal 23: 79-81.

[5] Swatland, H.J. (1995). Reversible effect on pork paleness in a model system. Journal of Food Science 60: 988-991.

[6] De Sénarmont, H. (1840). Sur les modifications que la réflexion spéculaire à la surface des corps métalliques imprime à un rayon de lumière polarisée. Annales de Chimie et de Physique 73: 337-362.

[7] Goranson, R.W. and Adams, L.H. (1933). A method for the precise measurement of optical path-difference, especially in stressed glass. Journal of the Franklin Institute 216: 475-504.

[8] Hartshorne, N.H. and Stuart, A. (1970). Crystals and the Polarising Microscope. 4th edit., Edward Arnold, London. pp. 308-318.